parametric imaging, MRI,
IR thermal imaging, image registration

Jacek RUMIŃSKI*, Marek SUCHOWIRSKI*

APPLICATIONS OF IMAGE REGISTRATION IN PARAMETRIC IMAGING

Applications of image registration in parametric imaging are investigated. The manual and automatic image registration methods have been used for image to image registration in sequences to correct movement artefacts in reconstructed parametric objects. Additionally the registration methods were used for multimodal visualisation of structural and parametric objects. The achieved results proved that the automatic image to image registration, for motion mechanisms correction, in the parametric model improves the quality of images. The multimodal visualisation of structural MRI images and parametric DSC-MRI images, enables to correlate the local dynamic changes with all morphological features.

1. INTRODUCTION

Parametric images represent values of reconstructed parameters for an assumed tissue/activity model. This extends the structural imaging towards functional imaging, e.g. Dynamic Susceptibility Contrast DSC-MRI [1], ASL MRI [2], dynamic PET/SPECT [3], active thermography [4], etc.

In parametric imaging studies we assume that the state of the object is modified based on internal or external excitations (natural or artificial). The chosen property or a set of properties are measured as the excitation related responses of the object. In these studies a set of images (sequence) is measured; each for a particular time point; assuming regular or irregular sampling rates. Every 1D signal is characterised by its location (p-pixel index) and a set of samples:

$$S^p = \left\{ s_1^p, s_2^p, s_2^p, .., s_K^p \right\}, \qquad (1)$$

where: K – is a total number of samples measured during a dynamic study, p – index of a measurement point, related to *(x,y)* coordinates.

Based on observations and/or other knowledge the object/process model is assumed. The model is characterised by a set of parameters. The task is to find for each S^p appropriate (the possible best) set of parameters. Synthesis of parametric images usually uses model to data fitting procedures or matrix-based operations. The calculated parameter value for each S^p generates a matrix, used for parametric image composition. Depending on chosen object/process model a set of parametric images can be generated. In this study we used

* Department of Biomedical Engineering, Gdansk University of Technology

parametric images for active, dynamic infrared imaging (ADIR) and dynamic susceptibility contrast (DSC) MRI visualisation.

2. PARAMETRIC IMAGING

In the active, dynamic infrared imaging a target object is excited (fan cooling, optical heating - used in the reported study) during a given time period Δt. As a result of the heating the object temperature varies in time according to thermal properties of the object. Sequence of images is recorded by thermal camera with frequency adjusted to the object properties and heating conditions. The observed character of time series is exponential and can be described by the formula:

$$\hat{s}_i^p = B_0^p + \sum_{j=1}^{N} B_j^p * \exp\left(-\frac{t_{i-1}}{\tau_j^p}\right); \mathrm{i} = 1..\mathrm{K} \qquad (2)$$

where: B – amplitudes, $\hat{s}_i^p$ - analytical value of a i-th sample (estimate), N – number of time parameters (none layers of equivalent electrical RC model), $\tau_j{}^p$ - time constant for layer j.

We explore one and two layers models (parameters: B_0 and up to two time constants A1= B_1^p , A2=1/ τ_1^p , A3= B_2^p , A4=1/ τ_2^p).

The described parameters represent thermal properties of the object (that are related to conductivity, heat capacity, etc.). Parametric image reconstruction method is looking for parameters of the equation (2), which minimise fitting errors to the measured set of samples (1). ADIR imaging was used to investigate this new method for skin burns investigation. Images were collected during phantom and in-vivo (domestic pig) studies. In the applied ADIR imaging the optical heating (a set of lamps - 1000W) was usually lasting 30s. Thermal images were captured every 1s during 90-180 seconds (up to 90-180 images, K=90-180).

Three different phantoms and three domestic pigs were used. The Local Ethics Commission approved the plan of experiments conducted on young pigs.

In DSC-MRI imaging, after injection of a bolus of contrast agent (e.g. Gd-DTPA), a series of images are measured. This image-sequence data presents local voxel activity of contrast (blood) flow and distribution. It is assumed, that measured MRI signal values are proportional to the contrast concentration. Contrast concentration as a function of time is measured for brain supported arteries which is estimated as the arterial input function (AIF). In real conditions the AIF is not an ideal impulse function (dispersion and delay), additionally in DSC-MRI measurements are done from a volume of interest (VOI) therefore deconvolution is required to calculate VOI impulse response *F*R(t)*:

$$C_t(t) = \frac{\rho}{Kh}\int_0^t C_a(\tau)\cdot\left(F\cdot R(t-\tau)\right)d\tau \qquad (3)$$

where: $C_a(t)$ - contrast concentration in the artery (e.g., Middle Cerebral Artery) – Arterial Input Function AIF, $C_t(t)$ - contrast concentration in the tissue, $\frac{\rho}{Kh}$ - scaling factor (quantitative description), *F*R(t)* – scaled impulse response (residue function) inside VOI. The *R(t)* - represents fractional tissue concentration.

Assuming that contrast material remains intravascular and the first pass of the contrast bolus can be eliminated from the concentration function a set of perfusion related parameters can be calculated (using deconvolution to find *R(t)*). Since *R(t=0)* should be equal to 1, then

$$F \cdot R(t=0) = F = rCBF \text{ (regional Cerebral Blood Flow).} \qquad (4)$$

Regional cerebral blood volume (proportional to the normalised total amount of tracer) and mean transit time (average time required for any given particle of tracer to pass through the tissue after an ideal bolus injection) can be estimated as:

$$rCBV = \left(\int_0^\infty C_t(\tau) d\tau \right) / \left(\frac{\rho}{Kh} \int_0^\infty C_a(\tau) d\tau \right); \; rMTT = rCBV/rCBF. \qquad (5)$$

Image sequences for in-vivo measurements were collected using 1.5T MRI scanner (SE-EPI with: 12 slices, 50 samples, TR=1.25-1.61s; TE=32-53ms; slice thickness 5-10 mm; 60 series - 3000 images). Using own, created software (by Java) we extracted signals and concentration curves used in further processing to reconstruct rCBF, rCBV and rMTT parametric images.

3. GEOMETRY TRANSFORMATIONS

Global and local geometry transformation methods were investigated. In case of global geometry transformations the affine transformations and non-linear transformations (i.e. polynomial transformations) were analysed and implemented. Finding appropriate control global point pairs it is possible to automatically calculate transformation parameters and use them for an image geometry transformation. Local geometry transformations were tested for the Delaunay triangulation and for the morphing transformation (based on image morphing). Morphing transform is based on the line segment comparison between template and transformed images. Detail description of the method was presented in [5].

In image registration the very important problem is to find corresponding pairs of control points (CPs). The simplest method is to find manually as many CPs as required for a particular registration algorithm. Another possibility is to develop an algorithm for automatic identification of CPs in source and target images. In literature there are many reviews of algorithm for automatic registration of images (e.g. [6][7][8]). Usually, those methods are dedicated solutions for given class of images.

In this study we developed methods for automatic identification of CPs for two basic goals in the parametric imaging process:

1. geometry correction due to patient (animal) movements during dynamic experiment;

2. multimodal visualisation of structural and parametric images.

Three software packages were implemented in Java programming language for image registration/multimodal visualisation, parametric image reconstruction for ADIR imaging and DSC-MRI. The implemented methods for image registration and multimodal visualisation support a user with opportunity to read source/target images (DICOM and other formats), perform manual CPs identification, automatic CPs identification, image registration with specified method (global or local), and multimodal visualisation using alpha-blending globally or within ROI. Automatic identification of CPs is implemented differently for movements' correction (MC) in an image sequence and for multimodal visualisation.

In case of MC the images were filtered by threshold to find regions. Those regions are used as masks to correlate their interior values between images *i* and (*i+1*) in a sequence. Since images in a one sequence present the same objects in time, they are very similar. Therefore the pattern matching method is used testing different locations (and it's local neighbourhood) to compare nearest regions in corresponding images (i.e. image *i* and *i+1*). As the similarity measure the correlation coefficient is used (similar range of values). The decision about which CP should be used is based on correlation coefficient value and a distance between the reference CP in *i*-th image and candidates in image no *i*+1. The CP is a region centre of gravity.

In case of image registration for multimodal visualization either manual or automatic method for identification of CPs is used. In case of automatic method image color tables are compared and fitted (a greyscale colour table M2-black-to-white is used). Then images are filtered by threshold (using automatic threshold estimation based on local gradients) and the surrounding background is eliminated using image binarysation. Separate points elimination (high frequency noise is eliminated) is performed using morphological closing operator. The next step eliminates a scalp and bones (if present). The automatic method is used based on gradient difference in threshold source/target image. Then four characteristic points (edge points) are detected at North, South, West and East of the source/target image. In the next step the image is scanned top-down and left-right to find the external inner border points of threshold regions (e.g. of brain). The final set of points is reduced (if required) by eliminating those points which are not appropriate for a chosen registration method (e.g. points which are close each other). Farther the multimodal image is presented using global or local (i.e. inside a ROI) alpha blending:

$$c=(1-alpha)*a + alpha*b, \qquad (6)$$

, where: *c* – new pixel value, *a,b* – pixel values for a source image *a* and a target image *b*, *alpha* – scaling factor (0..1).

The alpha scaling factor, the ROI size and position can be defined using a graphical user interface created in Java programming language.

4. RESULTS, DISCUSSION AND CONCLUSION

The image sequences were process to reconstruct parametric images. First, the image to image registration was performed to correct patient (animal) movements. The most

representative examples can be presented for animal studies since there is very difficult to immobilize them. For particular sequences measured with ADIR imaging method the parametric images were calculated, first for non corrected sequences, then for corrected sequences. In most examples (were the observed movement was significant) we observed the improvement of quality in observed burned wounds (Fig. 1).

The image to image registration used in ADIR imaging improves the final result of parametric image reconstruction. The movement artefacts are highly reduced and the interested regions (burn wounds) are presented with more clear borders. In Fig. 1 it is easy to analyse the A1 parameter change in 4 burn wounds and used this information for decision taking about possible spontaneous healing of particular wounds. The quantitative results of the ADIR imaging diagnostic value in burn wounds investigation without motion correction (analysis by values averaging in a wound ROI) are presented in [4]. The application of motion correction eliminates the requirement of values averaging with a ROI and additionally improves quality of diagnostic (parametric) images. In Fig. 2 some results for image registration and multimodal visualization are shown. Automatic image registration for multimodal visualization was validated using experts (radiologists) opinions and based on experiments with a test set. Using original set of images a series of geometrically modified images was generated. MRI images were modified by eleven different affine and perspective transformations. The total number of images in a test set was 24. All images from a test set were processed to fit reference images using affine transformation, Delaunay triangulation and morphing transformation. As a measure of registration quality a difference image (i.e. registered compared to an original image before modifications) was generated. Difference images were constructed using greyscale. For quantitative evaluation of algorithms three indexes were used: RMS error (normalized to the dynamic range of image values), correlation coefficient and normalized standard error (NMSE) given as

$$NMSE = \frac{\sum_{x=0}^{X}\sum_{y=0}^{Y}\left(f(x,y) - f'(x,y)\right)^2}{\sum_{x=0}^{X}\sum_{y=0}^{Y}\left(f'(x,y)\right)^2} \qquad (7)$$

where: $f(x,y)$ – registered (transformed) image value for (x,y); $f'(x,y)$ – original (test set) image value for (x,y).

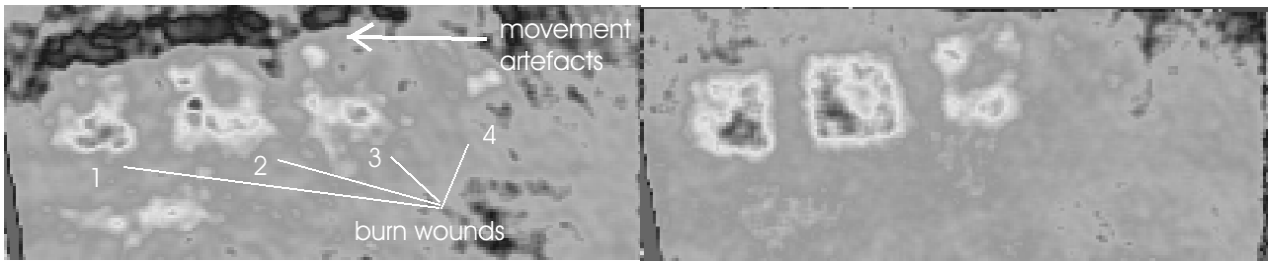

Fig.1 The ADIR A1 parametric image reconstructed for left: non corrected sequence, right: corrected sequence

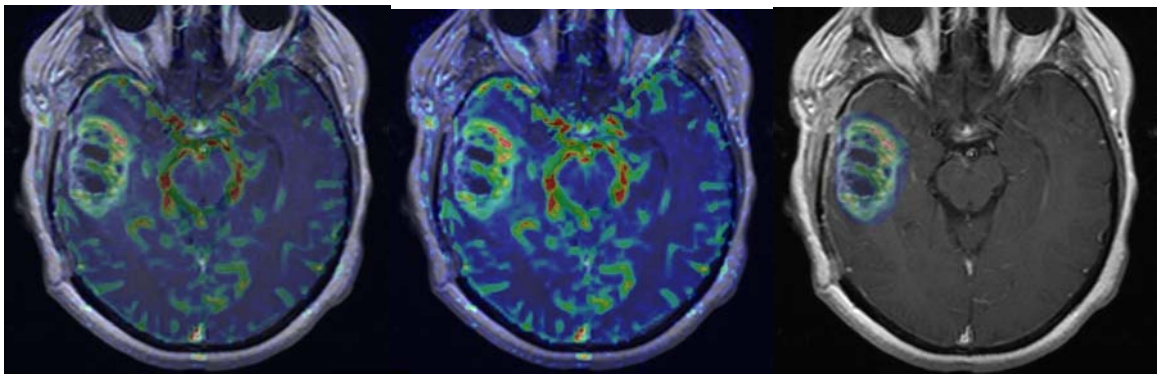

Fig. 2. The multimodal visualization of T1-weighted image and regional CBF image. Global and local alpha blending results are presented (high perfusion in the tumor region)

Taking into account all tests, the affine transform gave the worst results. It could be expected since affine transform is based on 3 global CPs only. Using triangulation of Delaunay, much better results were achieved. Of course, higher number of triangles (control points) leads to better normalization quality. However using automatic method (without artificial markers) it is very difficult to find many control points. In many cases morphing transform produced much better results than Delaunay transform. This is highly related to the compared objects sizes – if two objects were similar (in case of scale) then the morphing method worked more accurately. Some examples of results are presented in Fig. 3 and in Tab. 1. All methods were implemented in Java programming language. Tests were performed on Pentium 4 3.2GHz, 2GB RAM, Windows XP. Average calculation time results are 3.5s for affine transform, 6.2s for Delaunay transform and 12.5s for morphing transform.

Table 1. Examples of quantitative comparisons of original and automatically registered images from the test set (Fig. 3.)

	Normalized RMS (0 – the best)	NMSE (0 – the best)	Correlation coefficient (1 – the best)
Affine	0.0363	0.1506	0.868
Delaunay	0.0348	0.140	0.8769
Morphing	0.0357	0.147	0.871

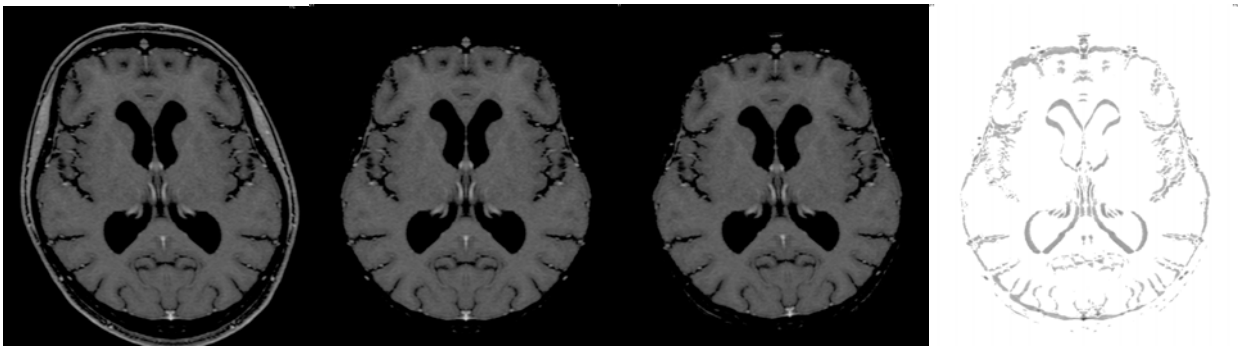

Fig. 3. Results of automatic image registration, form left: an example from the test set, original image (without scalp), automatically registered image, difference image (quantitative comparison in Tab. 1.)

Concluding, the automatic image to image registration for motion correction in ADIR imaging highly improved the quality of parametric images. The multimodal visualization of

structural MRI images and parametric DSC-MRI images enables to correlate local dynamic changes with morphological features. Further studies will investigate other automatic methods for image registration and the quantitative correlation of PET and DSC-MRI dynamic studies (e.g. CBF).

ACKNOWLEDGEMENT

The work was partially supported by the Polish State Committee for Scientific Research, grant No 4 T11E 042 25, 2003-2006. The authors would like to thank Barbara Bobek-Billewicz and Center of Oncology in Bydgoszcz for their cooperation on MRI/PET analysis and support.

BIBLIOGRAPHY

[1] Calamante F., Gadian D.G., Connelly A., Quantification of Perfusion Using Bolus Tracking Magnetic Resonance Imaging in Stroke. Assumptions, Limitations, and Potential Implications for Clinical Use, *Stroke*.;33:1146-1151, 2002.
[2] Wang J., Alsop D. C., Li L., Listerud J., Gonzalez-At J. B., Schnall M. D., Detre J. A., Comparison of Quantitative Perfusion Imaging Using Arterial Spin Labeling at 1.5 and 4.0 Tesla, MRM 48:242–254, 2002.
[3] Cai W., Feng D. D., Fulton R., Content based retrieval of dynamic PET functional images, IEEE Transactions on Information Technology in Biomedicine 4 (2)152-158, 2000.
[4] Rumiński J., Kaczmarek M., Nowakowski A., Medical Active Thermography – A New Image Reconstruction Method, LNCS2124, Springer,2 74-281, 2001.
[5] Rumiński J., Stachowiak T., Bobek-Billewicz B., Suchowirski M., MRI to PET-CT co-registration and differential analysis, EMBEC'05, IFMBE Proc., Prague, CD-edition, 6 pages, 2005.
[6] Elsen P.A. van den, Pol E.J.D., Viergever M.A., Medical image matching - a review with classification. IEEE Engineering in Medicine and Biology, 12(4):26-- 39, 1993.
[7] Maintz J., Viergever M., A Survey for Medical Image Registration. Medical Image Analysis, 2:1-36, 1998.
[8] Zitova B., Flusser J.,Image registration methods: a survey, Image and Vision Computing, Vol. 21, No. 11, pp. 977-1000, 2003.